DIRECTIONAL TUNING CURVES, ELEMENTARY MOVEMENT DETECTORS, AND THE ESTIMATION OF THE DIRECTION OF VISUAL MOVEMENT

J. H. VAN HATEREN

Department of Biophysics, University of Groningen, Westersingel 34, NL-9718 CM Groningen,
The Netherlands

Abstract—Both the insect brain and the vertebrate retina detect visual movement with neurons having broad, cosine-shaped directional tuning curves oriented in either of two perpendicular directions. This article shows that this arrangement can lead to isotropic estimates of the direction of movement: for any direction the estimate is unbiased (no systematic errors) and equally accurate (constant random errors). A simple and robust computational scheme is presented that accounts for the directional tuning curves as measured in movement sensitive neurons in the blowfly. The scheme includes movement detectors of various spans, and predicts several phenomena of movement perception in man.

Visual movement detection   Directional tuning curves   Blowfly   Reichardt correlator   Gradient
scheme   Apparent motion

INTRODUCTION

A visual movement detector that is directionally selective can be characterized by its directional tuning curve. This curve is the sensitivity of the detector as a function of the direction of movement. It is maximal in the preferred direction of the detector, and usually becomes smaller the more the direction of movement deviates from the preferred one. The response of visual movement detectors generally depends on other factors as well, such as the spatial structure of the stimulus, its contrast, and its speed. Therefore, it is not possible to determine the direction of movement accurately from the output of a single detector: a given response may indicate a stimulus moving exactly in the preferred direction as well as a more effective stimulus moving in another direction. The direction can be obtained accurately, however, if two or more detectors are available with different orientations and overlapping tuning curves (Sutherland, 1961). If the detectors depend in the same way on stimulus properties as contrast and speed, the ratio of their responses will uniquely code the direction of movement.

The main topic of this article is the problem of how, and how accurate, the direction of movement can be inferred from the output of two or more differently oriented detectors. I will concentrate on the simplest case of broadly tuned detectors along only two preferred axes. This is a situation encountered e.g. in the vertebrate retina (Oyster, 1968) and in the brain of insects (e.g. Hausen, 1984). A system with narrowly tuned detectors in many directions is mentioned as well. I show that under certain conditions, that appear to be satisfied in the brain of the fly, detectors oriented along only two axes can yield isotropic directional estimates. By isotropic I mean that the estimate of the direction of movement is unbiased (i.e. without systematic errors) and equally accurate (i.e. with constant random errors) in any direction.

The second topic of this article is the question of how tuning curves having the abovementioned isotropic properties may be produced. In general, movement detectors with only two spatially identical inputs fail. I propose a computational model that accounts for the observed directional tuning curves in the brain of the blowfly, and that might be relevant as well for units encountered in the vertebrate retina (Oyster, 1968) and for some units in area MT of the vertebrate cortex (Movshon, Adelson, Gizzi & Newsome, 1986).

METHODS

Preparation

Experiments were performed on female blowflies, *Calliphora vicina*. Movement sensitive

neurons in the lobula plate were recorded from using standard extracellular recording techniques (see e.g. Schuling, Mastebroek, Bult & Lenting, 1989). With regular feeding of the animals recordings were stable for typically a few days. Variations in sensitivity were checked with regular control experiments, and were very limited. The optical quality of the eye was checked by observing the far field radiation pattern (Franceschini, 1975) using antidromic light. The pattern often began deteriorating after 2 or 3 days, upon which the experiment was stopped. Tuning curves were obtained from 10 movement sensitive neurons for various stimuli, all yielding very similar results.

Stimuli

The stimuli were generated on a computer controlled CRT (mean radiance $36 \, mW/(m^2sr)$, visual field $24° \times 24°$, frame rate 1 kHz, line width $0.12°$). Direction of movement was changed with a Dove prism. The position of the stimulus relative to the far field (which shows the sampling lattice of the eye) could be observed during the experiment (van Hateren, Hardie, Rudolph, Laughlin & Stavenga, 1989; van Hateren, 1986) using an image intensifier and a video camera. The stimulus sequence for Fig. 2 was 1.08 sec of movement in a preferred direction (a direction increasing the spike rate), 1.08 sec steady, 1.08 sec in a null direction (a direction suppressing the spike rate), and 1.08 sec steady. For each condition the response was defined as the average spike rate in the period 0.4–1.0 sec. For directional tuning curves typically 400 stimulus presentations in each direction were presented, with directions presented in random order.

RESULTS AND DISCUSSION

Estimating the direction of visual movement

As was mentioned in the Introduction, the direction of movement can be estimated from the responses of two or more differently oriented detectors with overlapping directional tuning curves. For the sake of simplicity, we will only deal with the problem of obtaining the direction from the responses of the two nearest detectors, i.e. those detectors with preferred directions closest to the direction of movement. The problem is depicted in Fig. 1(a). Can we obtain the direction of movement θ from the two shown detectors? The answer is obviously
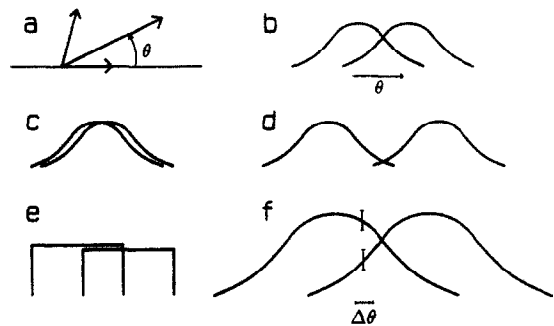

Fig. 1. Estimating the direction of movement with two differently oriented movement detectors with overlapping directional tuning curves. (a) The short arrows indicate the orientations (preferred directions) of two movement detectors, the long arrow indicates a direction of movement θ to be determined from the output of the detectors. Their sensitivities depend on the direction of movement as shown in (b) (directional tuning curves). The ratio of the curves yields information of θ. In (c) the tuning curves are too close together for reliable directional estimates, in (d) the region of overlap is too small. The tuning curves of (e) do not yield information on θ as their ratio is constant in the region of overlap. Noise in the tuning curves, as shown in (f), will lead to an uncertainty in the ratio of the two curves and thus to an uncertainty $\Delta\theta$ in the estimate of θ.

affirmative, if the ratio of their tuning curves, shown in Fig. 1(b), is unique for any direction in the region of overlap.

A second question is how accurate this estimate of direction will be. This depends on several factors, illustrated in Figs 1(c)–(f). Firstly, the overlap of the tuning curves is important. If the tuning curves are very close together, as in Fig. 1(c), a change in the direction of movement will hardly change the ratio of the detector responses, and the accuracy will not be high (unless more than two detectors are compared, the more complicated situation not considered in this article). If, on the other hand, the curves are far apart, as in Fig. 1(d), the direction can only be estimated in a very limited range. Clearly, in between these extremes there must be an optimum. Secondly, the shape of the tuning curves will be important. This is obvious from the example of Fig. 1(e): directions in the region of overlap can not be distinguished, as the ratio of the detector outputs does not change. Lastly, the amount of noise in the tuning curves is important: if both tuning curves fluctuate independent of each other, their ratio will fluctuate as well, and therefore the estimate of direction (Fig. 1f).

The following analysis quantifies the considerations given above. Suppose we have two local movement detectors, responding to movement in a small part of the visual field. We

assume that we can write the responses r_1 and r_2 of these local detectors as

$$r_1(\theta) = As_1(\theta), \qquad (1)$$

$$r_2(\theta) = As_2(\theta), \qquad (2)$$

with s_1 and s_2 only depending on the direction of movement θ, and A only on other factors, such as contrast and velocity of the stimulus. We further assume that s_1 and s_2 are independent of each other with variabilities Δs_1 and Δs_2 (possibly depending on θ), thus all the covariance of r_1 and r_2 is assumed to be due to A. We can now define a function f that eliminates A from equations (1) and (2)

$$f(\theta) = \frac{r_1(\theta)}{r_2(\theta)} = \frac{s_1(\theta)}{s_2(\theta)}. \qquad (3)$$

Given responses r_1 and r_2, we know the ratio s_1/s_2, and an estimate of θ follows from the inverse of f, assuming it exists

$$\theta = f^{-1}\left(\frac{s_1}{s_2}\right). \qquad (4)$$

Equation (4) is not intended as a model of how θ is inferred by the nervous system, but only as a means to determine how precisely information about θ is represented by the output of the two detectors. This information is already in a suitable form for further processing (in the spirit of the sensorium of Koenderink & van Doorn, 1987), eventually leading to motor output, and it is unlikely that there is somewhere during this processing an explicit calculation of θ. Nevertheless, all information on θ is represented by equation (4). The uncertainty in θ is

$$\Delta\theta = \sqrt{\left(\frac{\partial\theta}{\partial s_1}\Delta s_1\right)^2 + \left(\frac{\partial\theta}{\partial s_2}\Delta s_2\right)^2}$$

$$= \sqrt{\left(\frac{\partial f}{\partial s_1}\frac{d\theta}{df}\Delta s_1\right)^2 + \left(\frac{\partial f}{\partial s_2}\frac{d\theta}{df}\Delta s_2\right)^2}$$

$$= \frac{\sqrt{(s_2\Delta s_1)^2 + (s_1\Delta s_2)^2}}{|s_1's_2 - s_2's_1|}, \qquad (5)$$

where we used $d\theta/df = (df/d\theta)^{-1}$, and the prime denotes a derivative to θ. Thus if we know the directional tuning curves and the variability, equation (5) yields the accuracy with which θ can be obtained.

The analysis above assumes that s_1 and s_2 do not depend on the nature of the stimulus. If they do, another source of uncertainty will be introduced. In order to infer the direction of movement by comparing s_1 and s_2, some implicit assumption on the shape of s_1 and s_2 has to be made by the nervous system. If the stimulus happens to produce a different s_1 and s_2 than those assumed, this will lead to a (systematic) error in the estimate of θ. Although the nervous system could avoid this by using independent information on the structure of the stimulus, this would lead to complicated, noise enhancing computations. Therefore, it is important that s_1 and s_2 are as much as possible invariant for different stimuli.

In order to gain more insight in this matter, I measured directional tuning curves and response variability of wide-field neurons in the brain of the blowfly. These neurons are relatively easy to record from for long times, they can be identified uniquely from animal to animal (Hausen, 1984), and have properties virtually identical from animal to animal due to the fact that, by biological standards, the blowfly eye and brain are 'engineered' to a very high degree of structural and functional precision (see e.g. Franceschini, 1975; Strausfeld, 1976; Laughlin, 1987).

Directional tuning curves in the fly

The wide-field movement sensitive neurons in the lobula plate of the blowfly respond either to horizontal or vertical movement (Hausen, 1984). Figure 2(a) shows examples of directional tuning curves of two of these units, a horizontal one (H1, open circles) and a vertical one (V1, filled circles). The stimulus was a drifting square-wave grating, presented in the frontal part of the visual field. There the preferred directions of the horizontal and vertical neurons are very close to perpendicular; more to the periphery of the visual field the axes become more skew (Hausen, 1984). We will concentrate here on the simplest case of perpendicular axes, though the theory developed above may be applied to systems with skew axes as well. The neurons are directionally selective: movement in the preferred direction increases the spike rate, whereas movement in the null direction decreases the spike rate, suppressing the spontaneous activity (scaled to zero in Fig. 2). The curves of both neurons are well described by cosine functions (continuous curves in Fig. 2a) with different amplitudes in preferred and null directions, as was previously shown (Srinivasan & Dvorak, 1980; Hausen, 1982; Eriksson, 1984).

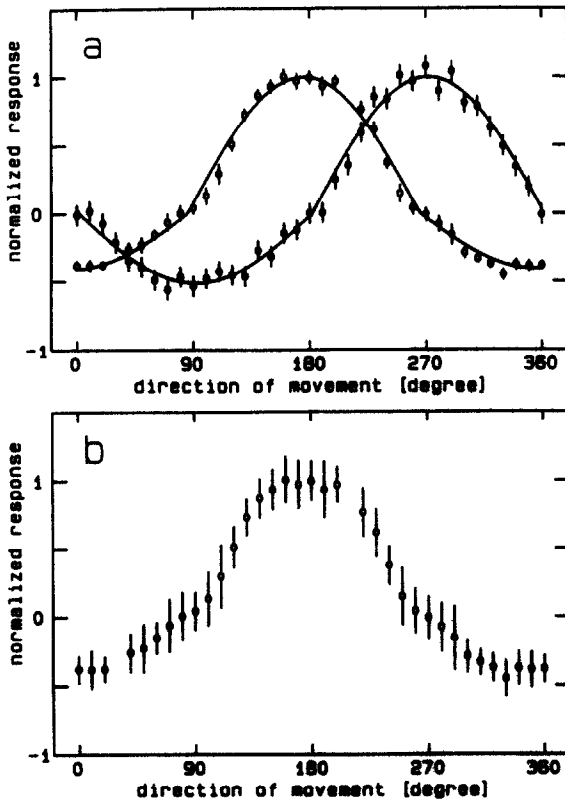One remarkable property of these neurons is that the shape of their tuning curves is very

Fig. 2. Directional tuning curves of neurons in the lobula plate of the blowfly. (a) Directional tuning curve of an H1 neuron, directionally selective to horizontal movement (open circles), and a V1 neuron, directionally selective to vertical movement (filled circles). The neurons were recorded from different animals. The stimulus was a drifting square-wave grating (speed $46.15°/sec$, temporal frequency 3.85 Hz, spatial wavelength $12°$, contrast 0.6 for H1 and 0.4 for V1) generated on a CRT (see Methods). Direction of movement was controlled with a Dove prism, angles are given relative to the horizontal axis of symmetry of the far field radiation pattern. The interommatidial angle $\Delta\varphi$ was $1.76°$ for H1 and $1.55°$ for V1. See Methods for the stimulus protocol and a definition of the response. Data points show normalized averages of 400 stimulus presentations in each direction; 0 is the response to the steady stimulus of the stimulus protocol (23 spikes/sec for H1, 12 spikes/sec for V1), 1 is the maximum response in the preferred direction (74 spikes/sec for H1, 34 spikes/sec for V1). Error bars show errors obtained from the standard deviation of the mean of responses to control stimuli repeated during the experiment. (b) Measurement of (a), H1 neuron, the error bars show the standard deviation of the responses, a measure of the response variability from trial to trial.

robust, i.e. the curves are essentially independent of the spatial structure of the stimulus. I obtained similar tuning curves for stimuli of different contrasts, different spatial wavelengths, different speeds, moving sinusoidal gratings, moving contrast borders, and different sizes of the stimulus. Eriksson (1984) obtained similar curves for a single moving spot.

Nevertheless, we can not use the tuning curves of Fig. 2(a) as the functions s_1 and s_2 needed for equation (5) without making some assumptions. The neurons recorded from are wide-field units, and, though they are exquisitely sensitive to local movement, they integrate movement information over a large part of the visual field. The theory developed in the previous section basically aims at giving information on local movement, given the responses of local, small-field movement detectors (though it can be applied to large-field units with exactly overlapping receptive fields as well). For the following, we will assume that the curves obtained from the large-field units reflect the properties of the underlying local subunits.

A second assumption concerns the different response amplitudes in preferred and null directions. This may reflect a similar asymmetry in the underlying subunits, but it seems more likely that it is due to the properties of the wide-field neurons themselves, as a similar asymmetry is seen in neurons being sensitive in the opposite direction (Hausen, 1984). We will therefore assume that the local subunits are bidirectional, i.e. have equal, but opposite responses in preferred and null directions. An alternative is that they are composed of identical, unidirectional movement detectors oriented in opposite directions and feeding with opposite signs into the wide-field neurons (e.g. Reichardt, 1969; see also Götz & Buchner, 1978). Thus we assume

$$s_1(\theta) = \cos\theta, \qquad (6)$$

$$s_2(\theta) = \sin\theta. \qquad (7)$$

What is the uncertainty, Δs_1 and Δs_2, of these tuning curves? Figure 2(b) shows the response variability of the horizontal neuron of Fig. 2(a). Surprisingly, this variability is in good approximation independent of the direction of movement. Again, we cannot infer the Δs_1 and Δs_2 needed for equation (5) directly without making further assumptions. Firstly, the variability shown in Fig. 2(b) is the standard deviation of responses defined as the average spike rate in a time window of 600 msec (see Methods). The size of the standard deviation will clearly depend on the length of the time window. This is unlikely, however, to influence the independency of the variability as a function of the direction of movement, and we will assume it does not. Secondly, we assume that the spike rate represents a good measure of the response and variability of the neurons. Nevertheless, it

may be that another measure for the response and its variability is utilized by the nervous system (see e.g. de Ruyter van Steveninck & Bialek, 1988). Finally, the variability as shown in Fig. 2(b) is in fact the Δr of equation (1), thus consisting of a variability due to A (e.g. due to photon noise and to noise in the photo-receptors) and a variability due to s. Figure 2(b) shows Δr is approximately independent of the direction, the same is likely to be true for A, and it seems therefore not unreasonable to assume that Δs_1 and Δs_2 are independent of the direction of movement as well.

With the assumption $\Delta s_1 = \Delta s_2 = \Delta s$, and with equations (6) and (7), equation (5) yields

$$\Delta\theta = \Delta s \frac{\sqrt{s_1^2 + s_2^2}}{|s_1' s_2 - s_2' s_1|} = \Delta s. \qquad (8)$$

With Δs independent of θ, we find that $\Delta\theta =$ constant. Thus the accuracy of estimating the direction of movement is direction indepen-dent.

Isotropic directional estimates

In the previous section we have seen that cosine-shaped directional tuning curves with the right overlap lead to an accuracy in the estimation of the direction of movement inde-pendent of this direction. Moreover, the experi-mental finding that the shape of the curves is very much independent of the spatial structure of the stimulus means that the estimate of θ on the basis of equation (4) is unbiased for any direction. The estimate contains no systematic errors even without any further information on the stimulus (though the system obviously may suffer from the aperture problem, see e.g. Marr & Ullman, 1981). These two properties lead to a system that codes the direction of movement isotropically: despite the fact that two discrete, perpendicular detector units are utilized, the system performs equally well in any direction.

If, on the other hand, the tuning curves s_1 and s_2 would depend on the spatial structure of the stimulus, equation (4) would give systematic errors in the estimate of θ for some stimuli at least (see previous section). These errors could only be corrected if independent information about the spatial structure of the stimulus were available (Reichardt, Schlögl & Egelhaaf, 1988). In one of the sections below we will see how we can construct a movement detector with a stimulus independent tuning curve.

Figure 3(a) illustrates again the functions s_1 and s_2 we assumed. Figure 3(b) shows an alternative way of obtaining the same kind of information, again with horizontally and verti-cally oriented units. Here four unidirectional units are used rather than two bidirectional units. The number of independent units has to be doubled because otherwise the estimate of θ is not unambiguous. Because the shape and overlap of the directional tuning curves is still the same, the accuracy is again independent of direction.

Figure 3(c) shows the tuning curves of Fig. 3(b) in a polar plot. Interestingly, this may be close to the situation encountered in the on–off directionally selective movement sensitive ganglion cells in the vertebrate retina. In the rabbit, these cells are organized along approximately perpendicular axes (Oyster, 1968), and have tuning curves with roughly the shape of cosines (rabbit: Oyster, 1968; turtle: Ariel & Adolph, 1985). Deviations from the ideal cosine shape do not necessarily mean that the concepts developed in this article cannot be applied. Complete isotropy of the estimation of direction is obviously an idealization. It makes no sense, e.g. to make systematic errors due to nonideally shaped tuning curves [equation (4)] very much smaller than the random errors due to noise in the tuning curves [equation (5)]. Thus depending on the required precision of the system some of the requirements for complete isotropy may be loosened.

Similar tuning curves as in Fig. 3(c) have been observed in some neurons in area MT of the vertebrate cortex as well (Maunsell & Van Essen, 1983; Movshon et al., 1986). It is not clear, though, whether the tuning curves of these neurons are invariant with the spatial structure of the stimulus.

Finally, Fig. 3(d) shows a system with a much larger number of unidirectional units, with narrow, cosine-shaped directional tuning curves. Because again shape and overlap are identical as in the previous examples, the esti-mate of direction is again isotropic. Obviously, the accuracy of this scheme will be higher than that of Fig. 3(c) if each neuron has a given amount of noise. It is tempting to suggest that Fig. 3(d) may describe some of the rationale of the narrowly tuned units encountered in the vertebrate cortex. In this context it is worth-while to note that there is no specific assumption on what the functions s_1 and s_2 code for, apart from being functions of θ. This article concen-trates on the direction of movement, but alter-natively s_1 and s_2 might e.g. code the orientation
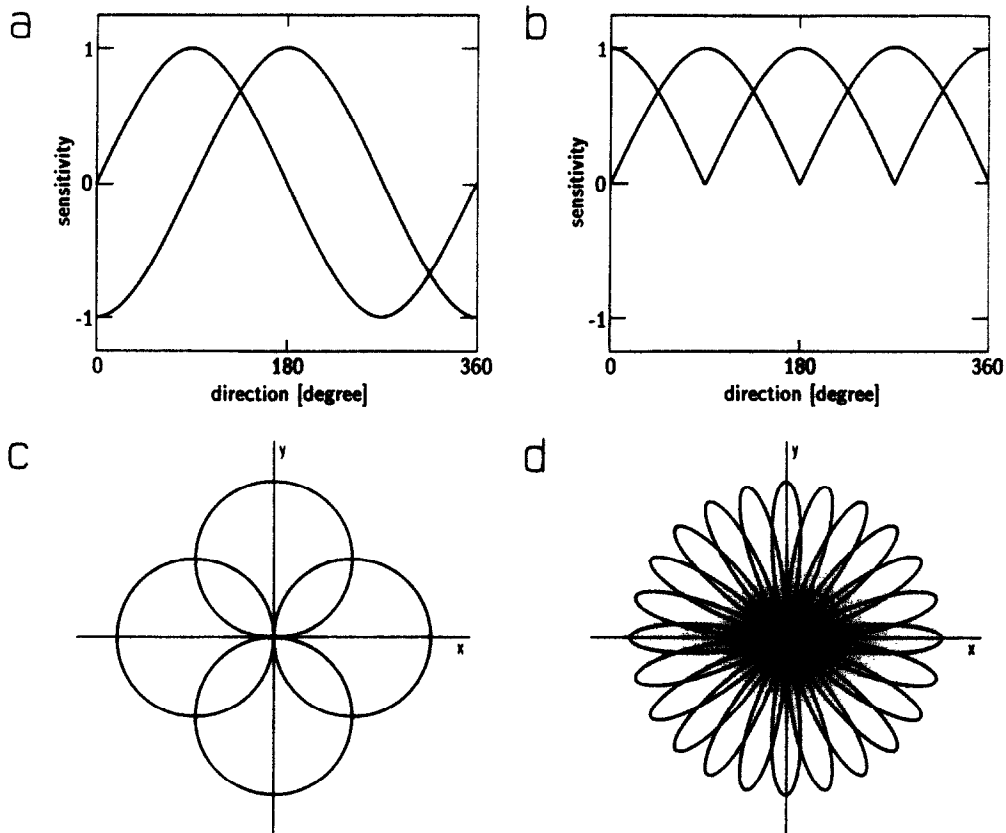
Fig. 3. Tuning curves yielding isotropic directional estimates. (a) Two neurons with bidirectional tuning curves. (b) Four neurons with unidirectional tuning curves, yielding equivalent information as in (a). (c) The tuning curves of (b) in a polar plot. (d) A polar plot of a system of 24 neurons with narrow unidirectional tuning curves. As the local shape and overlap of the neurons is similar to (c) (only scaled), the system still yields isotropic directional estimates. This system is more accurate than that of (c), given a certain noise level in each neuron.

of lines. Therefore, the theory may be applied as well to orientationally sensitive units not specifically sensitive to movement.

Let us go back to our starting point, Fig. 3(a). How do these curves compare to the tuning curves of some commonly used movement detectors?

Directional tuning curves of common movement detectors

First, consider the tuning curve of a detector that directly codes the speed it perceives along the line connecting its inputs. This type of detector may be considered as the one-dimensional implementation of the gradient scheme (Fennema & Thompson, 1979; Horn & Schunk, 1981). On first sight, one may assume that such a detector will perceive the component of the velocity vector along its main axis (i.e. $v_{perceived} = v \cos \theta$). Unfortunately, for moving gratings or moving edges the $v_{perceived} = v/\cos \theta$ (Zanker, 1988). The reader can check this by

considering the time, as a function of the direction of movement, it takes for an edge, moving with a given speed, to travel from input 1 to input 2. Thus this detector will respond stronger the more the direction of movement deviates from its main axis, and the perceived velocity will approach infinity if θ goes to 90° (Fig. 4, see also Zanker, 1990).

A second popular movement detector uses multiplication of suitably filtered inputs (Reichardt correlator, see e.g. Reichardt, 1969; van Santen & Sperling, 1985). Its spatial behaviour is governed by the so-called interference factor (Götz, 1964; van Santen & Sperling, 1985)

$$\sin\left(\frac{2\pi\Delta\varphi}{\lambda}\right),\tag{9}$$

with $\Delta\varphi$ the angular distance between its two inputs, and λ the (angular) spatial wavelength of the stimulus. Equation (9) is valid for stationary movement, for dynamic (i.e. starting, changing)
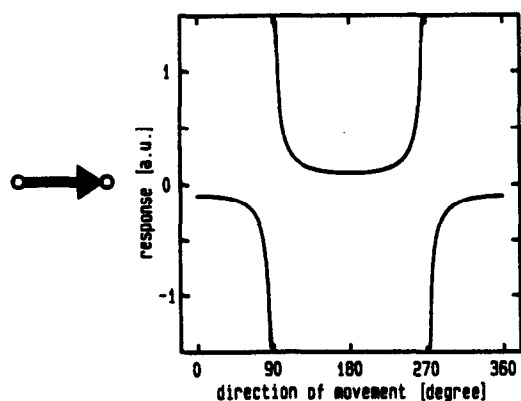
Fig. 4. The directional tuning curve of a movement detector responding proportional to the velocity it perceives along the line connecting its inputs (e.g. a one-dimensional implementation of the gradient scheme). The curve is given by $-0.1/\cos\theta$, with 0.1 an arbitrary scaling constant.
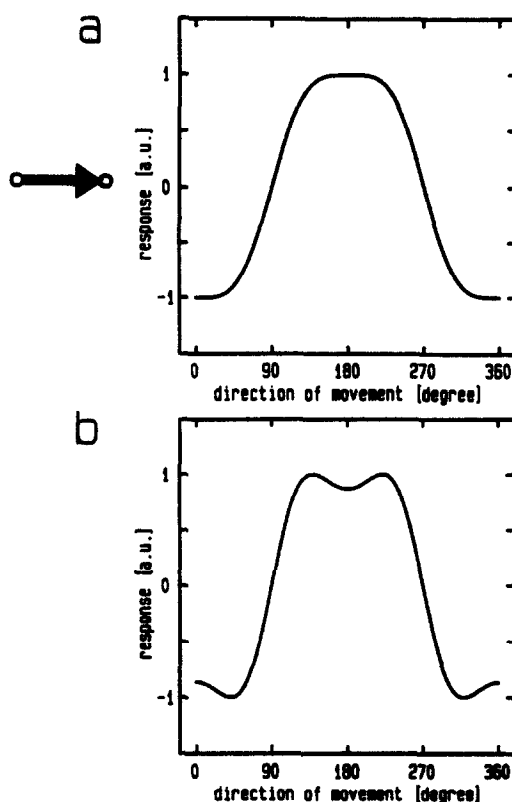

Fig. 5. Directional tuning curves of a multiplicative movement detector (Reichardt correlator), in (a) for the spatial wavelength optimally exciting the detector ($\lambda = 4\Delta\varphi$), and in (b) for a slightly smaller, but still quite effective wavelength ($\lambda = 3\Delta\varphi$). The curves are given by equation (10) (see text).

movement the situation may become more complicated (Egelhaaf & Borst, 1989). Other factors influencing the response of a multiplicative movement detector, such as the temporal frequency of the stimulus, and the spatial low-pass filtering due to the optics of the system, do not change as a function of the direction of movement. However, the spatial wavelength perceived by the detector along its axis changes as $\lambda/\cos\theta$, leading to a tuning curve given by (Zanker, 1988)

$$s(\theta) = c \sin\left(\frac{2\pi\Delta\varphi}{\lambda}\cos\theta\right), \qquad (10)$$

with c a normalization constant.

Figures 5(a) and (b) show the tuning curves of the multiplicative movement detector for two spatial wavelengths, the wavelength giving optimal responses ($\lambda = 4\Delta\varphi$, Fig. 5a), and a somewhat shorter wavelength ($\lambda = 3\Delta\varphi$, Fig. 5b). The tuning curve is much closer to the observed curves of Fig. 2 than the tuning curve of the velocity detector (Fig. 4), but it still has defects (Zanker, 1990). As Fig. 5(b) shows, it develops a minimum in its preferred direction for short spatial wavelengths, which I never observed in the directional tuning curves I measured. Although the detector will have a cosine-shaped tuning curve for $\lambda \gg \Delta\varphi$ (the sine in equation (10) can then be approximated by its argument) its main defect is that its shape depends on the spatial wavelength (Figs 5a and b). Thus the estimate of θ, following from equation (4), will be liable to large systematic errors (see the next section), depending on the spatial structure of the stimulus.

Concluding, we have seen that both detectors considered above do not perform very well. Thus we are left with the question of how we can construct a detector that does perform satisfactorily, i.e. produces cosine-shaped directional tuning curves for arbitrary stimuli. Fortunately, the answer is quite simple.

A computational model producing cosine-shaped tuning curves

A promising way to produce a cosine-shaped tuning curve is by orienting two (unspecified) movement detectors at 60° to each other, as shown in Fig. 6. This follows from the following symmetry arguments. In Fig. 6(a) the stimulus is moving horizontally, i.e. $\theta = 0°$. Both detectors, stimulated at 30°, will give equal contributions to the total response, which we arbitrarily set at 1. If the stimulus is now moving in a direction $\theta = 60°$ (Fig. 6b), one of the detectors is not stimulated, whereas the other is again stimulated at 30°. Therefore, the response will be 0.5 in this case. Finally, moving the
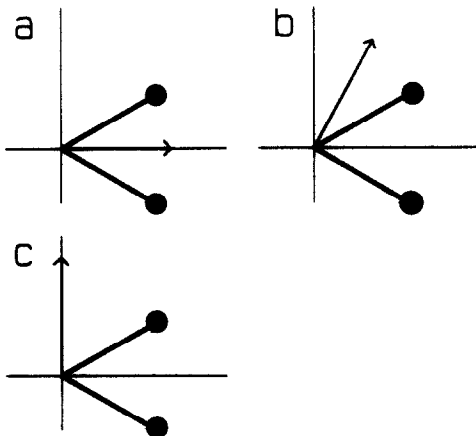
Fig. 6. Two detectors oriented at 60° to each other, with a common input at the origin. Simple considerations (see text) show that this configuration yields directional tuning curves equal to $\cos\theta$ at $\theta = 0°$, 60° and 90°, for any type of bidirectional detector.
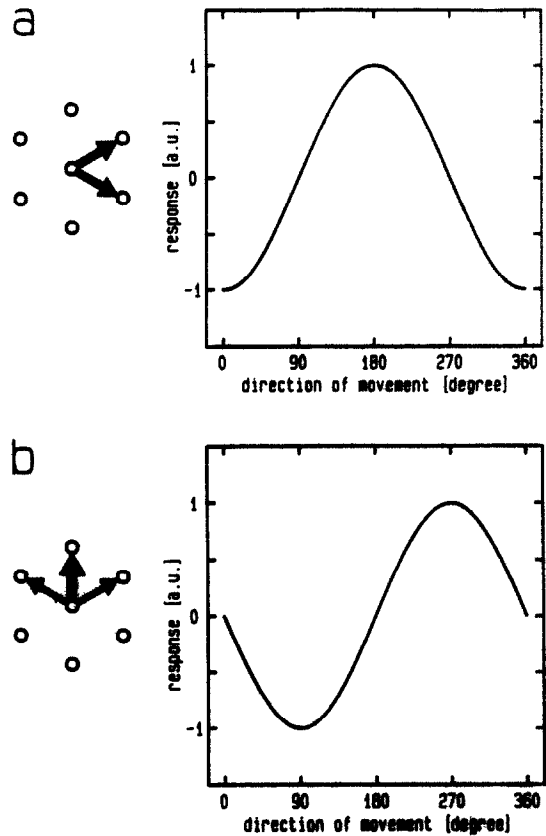

Fig. 7. (a) Directional tuning curve of a horizontally sensitive unit consisting of two multiplicative movement detectors differing 60° in orientation. The stimulus is a sinusoidal grating of wavelength $\lambda = 4\Delta\varphi$. The curve is given by equation (11), and is virtually identical to a cosine. (b) Tuning curve of a vertically sensitive unit consisting of three multiplicative movement detectors. Stimulus as in (a). The curve is given by equation (12), see text for further details and discussion.

stimulus in the direction 90° (Fig. 6c) will stimulate both detectors at 60°, but in opposite directions. Thus the total response will be 0 if the detectors are bidirectional. These simple considerations show that the response, independent of the type of the (bidirectional) detectors, will comply to $\cos\theta$ for $\theta = 0°$, 60° and 90°. As the sampling lattice of flies is hexagonal in good approximation (Franceschini, 1975), orienting the detectors at 60° to each other is a natural way of arranging them. In the frontal part of the visual field the hexagonal sampling lattice is oriented such that the hexagons are pointing upward and downward.

Figure 7(a) shows the performance of the configuration of Fig. 6 using multiplicative movement detectors (stimulus with $\lambda = 4\Delta\varphi$). A justification for using multiplicative movement detectors is that up till now this type of detector has been one of the most successful in explaining directionally selective movement sensitivity (Buchner, 1984; van Santen & Sperling, 1985). From equation (10) it follows that the tuning curve of Fig. 7(a) is given by

$$s(\theta) = -c\,\sin\left[\frac{2\pi\Delta\varphi}{\lambda}\cos(\theta - 30°)\right]$$

$$-c\,\sin\left[\frac{2\pi\Delta\varphi}{\lambda}\cos(\theta + 30°)\right], \quad (11)$$

with $c = 0.510$, a normalization constant found by fitting this function to $-\cos\theta$. The inference above that the angle α between the orientations of the detectors should be 60° was checked by fitting with α as another free parameter. The fit yielded $\alpha = 60.0°$, thus this value is indeed

optimal. The resulting tuning curve is very close to $\cos\theta$ for almost all λ (see below, and Zanker, 1990).

Figure 7(b) shows how a vertically sensitive unit can be constructed by using three multiplicative movement detectors. The curve (shown for $\lambda = 4\Delta\varphi$) is given by

$$s(\theta) = -c_1\,\sin\left[\frac{2\pi\Delta\varphi}{\lambda}\cos(\theta - 150°)\right]$$

$$-c_2\,\sin\left[\frac{2\pi\Delta\varphi}{\lambda}\cos(\theta - 90°)\right]$$

$$-c_1\,\sin\left[\frac{2\pi\Delta\varphi}{\lambda}\cos(\theta - 30°)\right], \quad (12)$$

with $c_1 = 0.294$ and $c_2 = 0.588$, found by fitting the function to $-\sin\theta$. That $c_2 = 2c_1$ in very good approximation follows also from the results of the horizontal scheme of Fig. 7(a): as

the curve of Fig. 7(a) is very close to cos θ, the unit effectively extracts from the movement the vector component along its preferred direction (Srinivasan & Dvorak, 1980). Therefore, the rules of vector addition apply, and the unit of Fig. 7(b) can be considered as the vector sum of two detector units of Fig. 7(a). A unit with an arbitrary preferred direction can be constructed by superimposing two detector units of Fig. 7(a) with suitable weights (given by the cosine of the angle between the desired preferred direction and the orientation of each detector, see also the Appendix).

These linear superpositions of differently oriented movement detectors yield directional tuning curves very close to cosines for most spatial frequencies. Only tuning curves for spatial wavelengths closely approaching the sampling limit of the lattice deviate ($\lambda \approx 2\Delta\varphi$). This hardly deteriorates the performance of the system, as these spatial wavelengths are attenuated by the properties of the multiplicative movement detector [equation (9)], and by the spatial low-pass filtering due to the optics of the eye (Götz, 1964; van Hateren, 1989). Equation (4) predicts that a combination of the units of Fig. 7 yields estimates of the direction of movement with systematic errors between 0.07° and 1.75° for the most effective spatial wavelengths (λ between $6\Delta\varphi$ and $3\Delta\varphi$), whereas this is between 2.9° and 15.5° for a combination of two dual-input movement detectors [as in Fig. 5, see equation (10)]. This calculation is based on the assumption that the nervous system implicitly assumes that s_1 and s_2 are given by cosine-shaped functions [equations (6) and (7)], i.e. the long-wavelength limits of equations (10), (11) and (12). The systematic errors increase the directional uncertainty due to random errors, as given by equation (5).

The theoretical tuning curves of Figs 7(a) and (b) were obtained for moving sinusoidal gratings. Tuning curves for arbitrary patterns will generally be similar, because the response of a multiplicative movement detector to a superposition of sinusoidal gratings of different spatial wavelengths equals the sum of the responses to each component separately (Poggio & Reichardt, 1973). As an arbitrary pattern can be thought of as a superposition of sinusoidal gratings (its Fourier components), its directional tuning curve will be the sum of the tuning curves of these sinusoidal gratings. With detectors oriented as in Fig. 7 it will be very close to a cosine. Of course, if the pattern is skew, i.e. if

its Fourier components are biased to one side with respect to the direction of movement, the tuning curve will be biased as well (the aperture problem).

The range of movement detection

The proposed schemes of Fig. 7 are consistent with results from behavioural experiments on flies (Buchner, 1976; Buchner, Götz & Straub, 1978). Other studies, however, indicate contributions also from other input pairs with longer ranges (Kirschfeld, 1972; Riehle & Franceschini, 1984; Schuling et al., 1989), especially in dark-adapted flies (Pick & Buchner, 1979). At first sight, including longer range interactions seems to lead inevitably to blurring, and therefore a decrease in the response to high spatial frequencies. This is not consistent with experimental findings: the resolution limit of the movement detection system in the fly is very close to that expected from next-neighbour interactions as in Fig. 7 (see e.g. Buchner, 1976). Figure 8 shows how this apparent paradox can be resolved, while maintaining the cosine-shape of the tuning curve.

Figure 8(a) shows again the scheme of Fig. 7(a). A similar set of detectors can be assumed to be pointing in the opposite direction. Now suppose we pool inputs, as suggested in Fig. 8(b) by the large circles. If a suitable weighting is chosen for this pooling, short spatial wavelengths will be strongly attenuated, whereas longer spatial wavelengths will encounter a system that is effectively identical to the one of Fig. 8(a), only with a longer range (or, of a larger spatial scale, see e.g. Koenderink, 1984). As the system still consists of two detectors at 60° to each other, the tuning curve will still be cosine-shaped and independent of the spatial structure of the stimulus. Figure 8(c) shows a similar arrangement with a still longer range and stronger pooling. Finally, in Fig. 8(d) these systems are superimposed. Short spatial wavelengths are ignored by the long range components of this system, but are seen by the short range components. The system will thus still respond well to these short spatial wavelengths, and have the high spatial resolution observed experimentally. The short range components of this system, on the other hand, will more or less ignore long spatial wavelengths because the phase-difference between the inputs then becomes small [see equation (9)]. Therefore, different parts of this system respond to different spatial frequency bands.
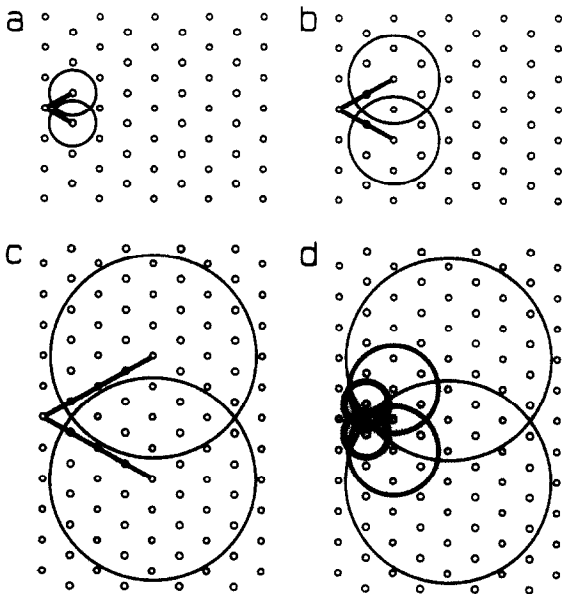
Fig. 8. The compatibility of long range interactions with high spatial resolution. (a) The scheme of Fig. 7(a), yielding robust directional tuning curves and high spatial resolution. The small circles represent inputs of the system (the sampling lattice), the fat lines two movement detectors. (b) Pooling of the inputs inside the large circles will abolish the response to the highest spatial frequencies. For lower spatial frequencies the system is functionally equivalent to the system of (a), only at a larger spatial scale. (c) As (b), at a still larger spatial scale. (d) The superposition of the schemes of (a), (b) and (c), assumed to be realized at the same time in a single movement detecting system. With suitable weights (suggested by the thickness of the circles), the system will respond to both high spatial frequencies and to low spatial frequencies moving at high speeds. See the Appendix for a mathematical foundation of this scheme.

Figure 8(d) is a superposition of three discrete systems, but we can make the transition to the continuous case as well, superimposing many subsystems with continuously varying range and resolution (this is put on a quantitative basis in the Appendix). Of course, I do not claim that the systems as in Fig. 8(d) are each present separately in the nervous system of the fly. Rather, they can be thought of as conceptual components of a single movement detecting system. This system pools the inputs, with suitable weights, before the multiplication, or, alternatively, pools the outputs, with suitable weights, of the various detectors. The amount of pooling may depend on the state of light adaptation (Pick & Buchner, 1979; Srinivasan & Dvorak, 1980; Schuling et al., 1989). The proposed scheme is similar to measurements of Pick and Buchner (1979) and of Schuling et al. (1989).

Interactions up to a certain limit (d_{max}) were also inferred for the human visual system as part of a low level, short range process (Braddick, 1974). A possible advantage of including long range interactions (still belonging to Braddick's short range process, not the long range process) is that they increase the velocity range of movement detection (Burr & Ross, 1982). Given a certain time course (delay or time constant) of the slow filter in the multiplicative movement detector, higher speeds can be perceived only if inputs are compared over longer distances. Figure 8(d) predicts that these high speeds can only be perceived with stimuli containing sufficiently long spatial wavelengths, which was indeed observed for the human visual system (Burr & Ross, 1982). Also, the dependence on spatial wavelength of both d_{max} (Chang & Julesz, 1983) and receptive field size (Anderson & Burr, 1987) follows naturally from Fig. 8(d).

CONCLUSION

In this article I showed how an isotropic movement detecting system can be constructed from detectors oriented along perpendicular axes. I also showed how these detectors can obtain the desired cosine-shaped and stimulus independent directional tuning curves from inputs located on a hexagonal sampling lattice. The system appears to be present in the eye of the blowfly, and may have been realized or approximated in other neural systems as well (vertebrate retina, area MT of the vertebrate cortex). Finally, I showed how long range interactions can be compatible with both well-behaved directional tuning curves and a high spatial resolution of the movement detecting system.

REFERENCES

Anderson, S. J. & Burr, D. C. (1987). Receptive field size of human motion detection units. *Vision Research, 27*, 621–635.

Ariel, M. & Adolph, A. R. (1985). Neurotransmitter inputs to directionally sensitive turtle retinal ganglion cells. *Journal of Neurophysiology, 54*, 1123–1143.

Braddick, O. J. (1974). A short-range process in apparent motion. *Vision Research, 14*, 519–527.

Buchner, E. (1976). Elementary movement detectors in an insect visual system. *Biological Cybernetics*, *24*, 85–101.

Buchner, E. (1984). Behavioural analysis of spatial vision in insects. In Ali, M. A. (Ed.), *Photoreception and vision in invertebrates* (pp. 561–621). New York: Plenum.

Buchner, E., Götz, K. G. & Straub, C. (1978). Elementary detectors for vertical movement in the visual system of *Drosophila*. *Biological Cybernetics*, *31*, 235–242.

Burr, D. C. & Ross, J. (1982). Contrast sensitivity at high velocities. *Vision Research*, *22*, 479–484.

Chang, J. J. & Julesz, B. (1983). Displacement limits for spatial frequency filtered random-dot cinematograms in apparent motion. *Vision Research*, *23*, 1379–1385.

Egelhaaf, M. & Borst, A. (1989). Transient and steady-state response properties of movement detectors. *Journal of the Optical Society of America*, *A6*, 116–127.

Eriksson, E. S. (1984). Vector analysis in a neural network. *Journal of Insect Physiology*, *30*, 363–368.

Fennema, C. L. & Thompson, W. B. (1979). Velocity determination in scenes containing several moving objects. *Computers and Graphics Image Processing*, *9*, 301–315.

Franceschini, N. (1975). Sampling of the visual environment by the compound eye of the fly: Fundamentals and applications. In Snyder, A. W. & Menzel, R. (Eds.), *Photoreceptor optics* (pp. 98–125). Berlin: Springer.

Götz, K. G. (1964). Optomotorische Untersuchung des visuellen Systems einiger Augenmutanten der Fruchtfliege *Drosophila*. *Kybernetik*, *2*, 77–92.

Götz, K. G. & Buchner, E. (1978). Evidence for one-way movement detection in the visual system of *Drosophila*. *Biological Cybernetics*, *31*, 243–248.

Gradshteyn, I. S. & Ryzhik, I. M. (1980). *Table of integrals, series, and products*. Orlando: Academic Press.

Hateren, J. H. van (1986). Electrical coupling of neuro-ommatidial photoreceptor cells in the blowfly. *Journal of Comparative Physiology*, *A158*, 795–811.

Hateren, J. H. van (1989). Photoreceptor optics: Theory and practice. In Hardie, R. C. & Stavenga, D. G. (Eds.), *Facets of vision* (pp. 74–89). Berlin: Springer.

Hateren, J. H. van, Hardie, R. C., Rudolph, A., Laughlin, S. B. & Stavenga, D. G. (1989). The bright zone, a specialized dorsal eye region in the male blowfly *Chrysomyia megacephala*. *Journal of Comparative Physiology*, *A164*, 297–308.

Hausen, K. (1982). Motion sensitive interneurons in the optomotor system of the fly. II. The horizontal cells: Receptive field organization and response characteristics. *Biological Cybernetics*, *46*, 67–79.

Hausen, K. (1984). The lobula-complex of the fly: Structure, function and significance in visual behavior. In M. A. Ali (Ed.), *Photoreception and vision in invertebrates* (pp. 523–559). New York: Plenum.

Horn, B. K. P. & Schunk, B. G. (1981). Determining optic flow. *Artificial Intelligence*, *17*, 185–203.

Kirschfeld, K. (1972). The visual system of *Musca*: studies in optics, structure and function. In Wehner, R. (Ed.), *Information processing in the visual system of arthropods* (pp. 61–74). Berlin: Springer.

Koenderink, J. J. (1984). The structure of images. *Biological Cybernetics*, *50*, 363–370.

Koenderink, J. J. & Doorn, A. J. van (1987). Representation of local geometry in the visual system. *Biological Cybernetics*, *55*, 367–375.

Laughlin, S. B. (1987). Form and function in retinal processing. *Trends in Neuroscience*, *10*, 478–483.

Marr, D. & Ullman, S. (1981). Directional selectivity and its use in early visual processing. *Proceedings of the Royal Society, London*, *B211*, 151–180.

Maunsell, J. H. R. & Van Essen, D. C. (1983). Functional properties of neurons in middle temporal visual area of the macaque monkey. I. Selectivity for stimulus direction, speed, and orientation. *Journal of Neurophysiology*, *49*, 1127–1147.

Movshon, J. A., Adelson, E. H., Gizzi, M. S. & Newsome, W. T. (1986). The analysis of moving visual patterns. In Chagas, C., Chagas, R., & Gross C., (Eds.), *Pattern recognition mechanisms* (pp. 117–151). New York: Springer.

Oyster, C. W. (1968). The analysis of image motion by the rabbit retina. *Journal of Physiology*, *199*, 613–635.

Pick, B. & Buchner, E. (1979). Visual movement detection under light- and dark-adaptation in the fly, *Musca domestica*. *Journal of Comparative Physiology*, *134*, 45–54.

Poggio, T. & Reichardt, W. (1973). Considerations on models of movement detection. *Kybernetik*, *13*, 223–227.

Reichardt, W. (1969). Movement perception in insects. In: Reichardt, W. (Ed.), *Processing of optical data by organisms and machines* (pp. 465–493). New York: Academic Press.

Reichardt, W., Schlögl, R. W. & Egelhaaf, M. (1988). Movement detectors provide sufficient information for local computation of 2-D velocity field. *Naturwissenschaften*, *75*, 313–315.

Riehle, A. & Franceschini, N. (1984). Motion detection in flies: Parametric control over ON–OFF pathways. *Experimental Brain Research*, *54*, 390–394.

Ruyter van Steveninck, R. R. de & Bialek, W. (1988). Real-time performance of a movement-sensitive neuron in the blowfly visual system: Coding and information transfer in short spike sequences. *Proceedings of the Royal Society, London*, *B234*, 379–414.

Santen, J. P. H. van & Sperling, G. (1985). Elaborated Reichardt detectors. *Journal of the Optical Society of America*, *A2*, 300–321.

Schuling, F. H., Mastebroek, H. A. K., Bult, R. & Lenting, B. P. M. (1989). Properties of elementary movement detectors in the fly *Calliphora erythrocephala*. *Journal of Comparative Physiology*, *A165*, 179–192.

Srinivasan, M. V. & Dvorak, D. R. (1980). Spatial processing of visual information in the movement-detecting pathway of the fly. *Journal of Comparative Physiology*, *140*, 1–23.

Strausfeld, N. J. (1976). *Atlas of an insect brain*. Berlin: Springer.

Sutherland, N. S. (1961). Figural after-effects and apparent size. *Quarterly Journal of Experimental Psychology*, *13*, 222–228.

Zanker, J. M. (1988). On the directional selectivity of motion detectors. *Perception*, *17*, A66.

Zanker, J. M. (1990). On the directional sensitivity of motion detectors. *Biological Cybernetics*, *62*, in press.

APPENDIX

Equation (10) gives the directional tuning curve of a single multiplicative movement detector. Suppose that a continuous field of movement detectors, with a central input common to all of them, is weighted according to

$$w(r)\cos \psi, \tag{A1}$$

with (r, ψ) polar coordinates centered around the common input. The tuning curve will be

$$s(f_s, \theta) = \int_0^\infty dr\, rw(r) \int_{-\pi}^{\pi} d\psi \cos \psi$$
$$\times \sin[2\pi f_s r \cos(\theta - \psi)], \quad (A2)$$

with $f_s = 1/\lambda$ the spatial frequency, θ the direction of movement, and r the continuous equivalent of the discrete $\Delta \varphi$ of equation (10). The integral over ψ can be evaluated by a change of variables $\beta = \psi - \theta$, a shift of the integration limits to $-\pi$ and π (allowed, because the integral goes over 2π), and an expansion of the first cosine. One of the resulting integrals equals zero (follows from symmetry), the other one is given by Gradshteyn and Ryzhik (1980,

equation 3.175.13). The result is

$$s(f_s, \theta) = \cos \theta\, 2\pi \int_0^\infty dr\, rw(r) J_1(2\pi f_s r)$$
$$= \cos \theta\, H_1\{w(r)\}, \quad (A3)$$

with J_1 a Bessel function of the first kind, and H_1 the first-order Hankel transform. Thus we get a cosine-shaped directional tuning curve if the angular weighting goes according to $\cos \psi$. The schemes of Fig. 7 are the simplest discrete approximations of this weighting. The spatial frequency response is given by the first-order Hankel transform of the radial weighting function $w(r)$. This leads to the possibility of quantifying and predicting the performance of systems as in Fig. 8(d).